arXiv:1211.1163v1 [quant-ph] 6 Nov 2012

Arbitrary quantum control of qubits in the presence of universal noise

Todd J. Green, Jarrah Sastrawan
Centre for Engineered Quantum Systems, School of Physics
The University of Sydney, NSW 2006 Australia

Hermann Uys
Centre for Scientific and Industrial Relations, Pretoria, South Africa

Michael J. Biercuk
Centre for Engineered Quantum Systems, School of Physics
The University of Sydney, NSW 2006 Australia

E-mail: `michael.biercuk@sydney.edu.au`

Abstract. In this manuscript we address the problem of deriving *analytic* expressions for calculating universal decoherence-induced errors in qubits undergoing arbitrary, unitary, time-dependent quantum-control protocols. For a qubit undergoing unitary decoherence the evolution of a qubit state in the presence of time-varying semiclassical fields may be treated geometrically. We show that the fidelity of an arbitrary control operation may then be expressed to arbitrary order in terms of experimentally relevant spectral characteristics of the noise and the control over all Cartesian directions and accounting for noise cross-correlations. We formulate *control matrices* in the time domain to capture the effects of piecewise-constant control, and convert them to generalized Fourier-domain filter functions. Such generalized filter functions may therefore be derived for complex temporally modulated control protocols, accounting for susceptibility to rotations of the qubit state vector in three dimensions. Taken together, this framework provides a computationally efficient means to calculate the effects of universal noise on arbitrary quantum control protocols without the need for time-consuming simulations of Bloch vector evolution. As a concrete example, we apply our method to treating the problem of dynamical decoupling incorporating realistic control pulses of arbitrary duration or form, including the replacement of simple π-pulses with complex dynamically corrected gates.

1. Introduction

The importance of efficiently controlling the evolution of a quantum coherent system has given rise to the development of the field of Quantum Control Theory [1, 2, 3, 4, 5, 6, 7]. Significant research attention has been devoted to this discipline due to the remarkable promise of quantum coherent technologies for future applications including quantum computation, quantum-enabled sensing, and quantum-enhanced metrology.

A primary challenge being addressed by the research community has focused on understanding and mitigating the deleterious effects of decoherence on quantum systems. In these processes, uncontrolled interaction with the environment leads to randomization of a quantum system's state, effectively destroying its "quantumness." This phenomenon is especially important in quantum information settings where net error rates deep below fault-tolerance thresholds ($\sim 10^{-4}$) are required in order to build scalable quantum computers [8].

A variety of methods have been developed to characterize the performance of quantum control protocols, with an eye towards estimating error rates due to decoherence in realistic, experimentally relevant noise environments which often have significant Non-Markovian characteristics. One of the most interesting from a practical perspective is the concept of *spectral overlap* formalized first by Kofman and Kurizki [9, 10]. In this general approach, the net susceptibility of a given quantum control protocol to environmental noise is given by the overlap in frequency between the environmental noise power spectral density and the spectral characteristics of the modulation imparted by the control.

These insights have been particularly important for the field of dynamical error suppression, which seeks to provide error robustness to quantum hardware at the physical level. These techniques address both implementation of memory or the identity (dynamical decoupling) [11, 12, 13, 14, 15] as well as nontrivial quantum logic gates (dynamically corrected gates) [16, 17] and exploit interference trajectories to effectively time-reverse the accumulation of error.

The concepts of the spectral overlap were expanded in the context of dynamical decoupling by Uhrig and Cywinski [18, 19], in attempting to understand the efficacy of these protocols in suppressing decoherence due to Non-Markovian environments. It was shown that, in considering DES broadly, the relevant control protocol could be thought of as a noise *filter*, and the efficiency of a particular control sequence deduced simply by an examination of the relevant filter transfer function [20]. This general approach has been repeatedly validated in experiments using a variety of technologies - from trapped atomic ions to semiconductor spin qubits [21, 22, 23, 24, 25]. Remarkable agreement has been demonstrated between simple theoretical expressions for error derived from the so-called "filter-function" and experimentally measured noise power spectra - so much so that inverting this approach has allowed DES protocols to be used in noise spectroscopy [26, 27, 28].

Despite these capabilities, there remains a significant gap in our understanding of how to efficiently calculate expected operational fidelities and error rates for complex quantum control protocols and for situations in which universal (i.e. multi-axis) time-dependent noise sources are present. For instance, relatively little is known about how to effectively account for the accumulation of error due to pulse non-idealities in dynamical decoupling sequences; the bang-bang limit is still widely assumed in analytic treatments.

Generally, while it is known that spectral overlap techniques may be employed in order to evaluate error rates, it is not known how to efficiently produce analytic filter functions appropriate for such complex quantum control protocols. This is largely due to that fact that the analytic complexity of deriving such functions grows significantly as soon as non-commuting operators appear in the control Hamiltonian - as would be the case in dynamical decoupling with nonzero-duration control pulses or other nontrivial control operations.

In this manuscript we address this challenge by developing a generalized method for evaluating the effects of universal, semiclassical decoherence on a quantum system undergoing an arbitrary unitary control protocol. By adapting the approach of Byrd and Lidar [29], to the case of bounded controls in a time-varying noise environment, we demonstrate how the effect of universal decoherence on an effective spin-1/2 qubit may be given to a geometric interpretation using a *control matrix*. In the presence of weak decohering noise, we show how all Cartesian contributions to the resulting entanglement fidelity may be calculated using noise power spectral densities and cross-power spectral densities along with the Fourier-space representations of the elements of the control matrix. Further, we show how it is possible to simply construct generalizations of the filter function for arbitrary control protocols by assuming piecewise-constant controls. As an example of the utility of this approach we study dynamical decoupling incorporating both realistic "primitive" π_X pulses and more complicated dynamically corrected gates. We are able to derive first order filter functions for the incorporation of arbitrary control pulses into a dynamical decoupling sequence and validate the performance of dynamically corrected gates in mitigating pulse errors in these sequences.

The remainder of the manuscript is organized as follows. In Sec. 2 we provide the relevant background to the problem of decoherence in qubits. This is followed by Sec. 3 which introduces the theoretical framework for quantum control in noisy environments and a geometric interpretation of decoherence, leading to the derivation of analytic expressions for the fidelity in Sec. 4. Sec. 5 then provides a concrete method to evaluate the control matrix (and hence the generalized filter functions) for the case of piecewise-constant control in the presence of universal and pure-dephasing noise. As an example demonstrating the practical utility of our method, this approach is applied to the problem of finite-pulse effects in dynamical decoupling in Sec. 6. Our framework permits us to efficiently separate out contributions to the filter function from the pulse *locations* from effects arising from the pulse *form* in a dephasing environment.

2. Background

A qubit is quantum system that exhibits two possible outcomes for the measurement of a particular physical observable: the z-component of the intrinsic angular momentum of a spin-1/2 particle being the archetypal example. Letting $|0\rangle$ and $|1\rangle$ denote the states in which one or other of these outcomes are returned with certainty, and assuming maximal knowledge of the system, an arbitrary qubit state may be written as a linear combination

$$|\psi\rangle = \cos(\vartheta/2)|0\rangle + e^{i\varphi}\sin(\vartheta/2)|1\rangle \tag{1}$$

The angles (ϑ, φ) define a three-dimensional unit vector, the Bloch vector, that provides a convenient pictorial representation of the state [8]. Interpreting all possible states geometrically in this way, the two-dimensional qubit state space is mapped to a sphere of unit radius, called the Bloch sphere (Figure 1).

The temporal evolution of the qubit is described by the propagator $U(t,0)$, a unitary operator that transforms some initial state $|\psi(0)\rangle$ to a final state $|\psi(t)\rangle = U(t,0)|\psi(0)\rangle$, for $t \geq 0$. The propagator satisfies the Schrodinger operator equation ($\hbar = 1$)

$$i\frac{d}{dt}U(t,0) = H(t)U(t,0) \tag{2}$$

where $H(t)$ is the Hamiltonian operator, which we assume to be traceless (i.e., $\mathrm{Tr}\,(H(t)) = 0$), for all t. Any solution to (2) may be written in the form $U(t,0) = \exp\left[-i\theta(t)\hat{\boldsymbol{n}}(t)\boldsymbol{\sigma}/2\right]$, where $\hat{\boldsymbol{n}}(t) = (n_x(t), n_y(t), n_z(t))$ is a real row vector of unit length, $\boldsymbol{\sigma} = (\sigma_x, \sigma_y, \sigma_z)^T$ is a column vector comprised of the Pauli spin operators, and $\theta(t)$ is a real function of time. The action of $U(t,0)$ on the state $|\psi(0)\rangle$ can then be thought of as a rotation of the corresponding Bloch vector through an angle $\theta(t)$, about an axis defined by $\hat{\boldsymbol{n}}(t)$. The set of all solutions to (2), in conjunction with the usual operator product, form a subgroup of the Lie group $SU(2)$ [30].

A basic requirement for the realization of a variety of quantum-based technologies, in particular quantum information processing (QIP) devices, is the capacity to manipulate coherent quantum states of the form (1) with a high degree of precision in the presence of uncontrolled environmental interactions. For a quantum system even relatively weak interactions with the environment can have a dramatic effect. An initially coherent quantum system S and its environment E become *entangled*, forming a single composite quantum system SE. From the perspective of an observer, with the capacity to measure only S, coherence is effectively lost [31]. If unaddressed, this process of *decoherence* can occur very rapidly, making the long term retention and accurate processing of information impossible.

In this work, rather than employ the full quantum-mechanical approach described above, we model the effect of the environment through a fluctuating classical noise field. Since the classical noise model and the purely quantum model of system-environment entanglement predict similarly negative impacts on the information processing capacity of a quantum system, we generically refer to both these processes as decoherence. The semi-classical approach has the advantage of not requiring a detailed knowledge of the system-environment interaction Hamiltonian. Further, it has been shown repeatedly that such phenomenological models can accurately represent important aspects of experimental reality [22].

3. Quantum Control in Realistic Environments

In this section we outline a mathematical treatment of a controlled quantum system affected by classical fields that serve to randomize the phase and probability amplitudes of a the quantum state, while preserving the vector norm (i.e. we omit leakage from the computational state space).

We consider an ensemble (either spatial or temporal) of identically prepared qubits, with dynamics determined by the single-qubit Hamiltonian $H(t) = H_0(t) + H_c(t)$. Here, the effect of the environment is modeled by the generalized noise Hamiltonian

$$H_0(t) = \boldsymbol{\beta}(t)\boldsymbol{\sigma} \tag{3}$$

where $\boldsymbol{\beta}(t) = (\beta_x(t), \beta_y(t), \beta_z(t))$ is a three-element row vector, each component of which is a random process modeling classical noise in one of the three spatial dimensions. Control over the state of the qubit can be achieved through the application of an external field, represented by

$$H_c(t) = \boldsymbol{h}(t)\boldsymbol{\sigma} \tag{4}$$

where the components of the vector $\boldsymbol{h}(t) = (h_x(t), h_y(t), h_z(t))$ describe the strength and direction of the control field as a function of time. We note that, for simplicity, we assume the all control is provided by $H_c(t)$, with no contribution from the internal qubit Hamiltonian.

3.1. Capturing the effects of time-dependent noise

As a brief qualitative illustration of the effect of noise on the capacity to manipulate the state of a quantum system, consider the application of a simple control Hamiltonian $H_c(t) = \Omega\sigma_x/2$ to an otherwise isolated qubit, where $\Omega \equiv \pi/\tau$ for some positive real number τ. Under these circumstances, the total Hamiltonian is independent of time and equation (2) is easily integrated to give $U(\tau, 0) = \exp[-i\pi\sigma_x/2]$. Thus, over a time interval $[0, \tau]$ the control field generates a rotation of the qubit Bloch vector through an angle of π radians (a 'π-pulse'), about the x-axis (Figure 1a). If we allow for nonzero but constant 'noise' by letting $\boldsymbol{\beta}(t) = (0, 0, \beta_z)$, for example, then $U(\tau, 0) = \exp[-i\pi(\sigma_x + \nu\sigma_z)/2]$, where $\nu \equiv 2\beta_z/\Omega$. The propagator now describes a rotation through an angle $\theta' > \pi$, about an axis that is tilted away from the xy-plane (Figure 1b). The noise therefore causes both a change in the angle of rotation and a shift of the rotational axis, so that the final qubit state will not be the one intended.

In most cases, deriving such a simple closed-form expression for the propagator $U(t)$ is not possible, as the Hamiltonian, in the presence of noise, will not generally

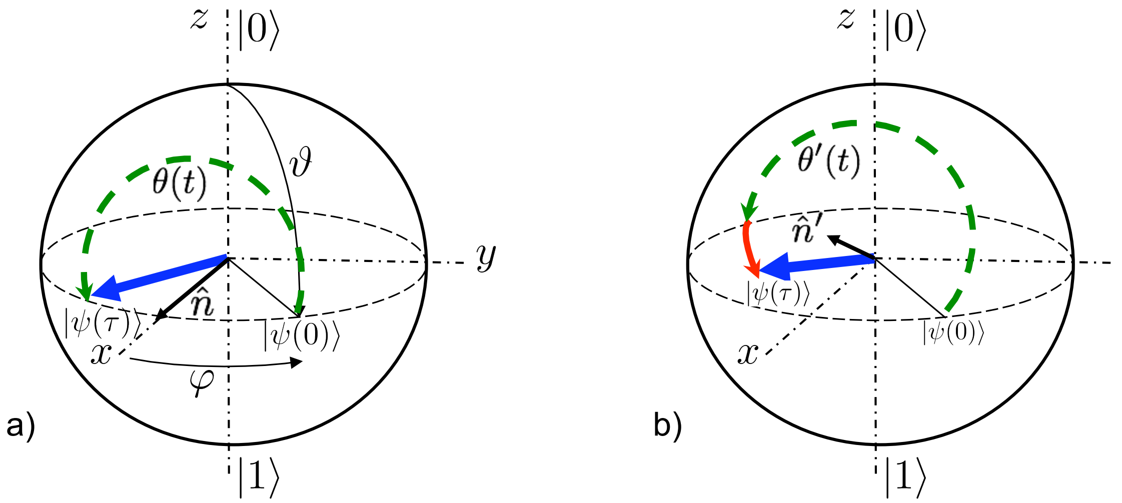

Figure 1. The Bloch sphere: showing a π-rotation about the x-axis, transforming an initial state $|\psi(0)\rangle$ to a final state $|\psi(0)\rangle$, for a) the ideal and b) the noise-affected control operations. The thick arrow indicates the final qubit state, the solid black arrow indicates the rotation axis, and the dotted path indicates the rotation angle. In b) the rotation axis and angle are both changed by the presence of the noise. Red extension of the path indicates overrotation in path $\theta'(t)$. See text.

commute with itself at different times (from here on, we omit the first argument of a propagator when it is zero). Therefore, rather than attempt to solve (2) directly, we introduce the 'control propagator' $U_c(t)$, defined as the solution to the *noise-free* Schrodinger equation $idU_c(t)/dt = H_c(t)U_c(t)$. We may then write $U(t) = U_c(t)\tilde{U}(t)$, with the 'error propagator' $\tilde{U}(t)$ capturing any deviation from the control evolution due to noise [32, 33]. Substituting $U(t) = U_c(t)\tilde{U}(t)$ into (2), and defining the 'toggling frame' Hamiltonian

$$\tilde{H}_0(t) \equiv U_c^\dagger(t)H_0(t)U_c(t) \tag{5}$$

we find that $\tilde{U}(t)$ satisfies the modified Schrodinger equation

$$i\frac{d}{dt}\tilde{U}(t) = \tilde{H}_0(t)\tilde{U}(t) \tag{6}$$

In the absence of noise, executing a target operation Q over a time interval $[0,\tau]$ simply requires one to engineer a control Hamiltonian such that $U_c(\tau) = Q$. Otherwise, the capacity to accurately 'steer' the qubit state via the control Hamiltonian $H_c(t)$ is reduced by the presence of the noise $H_0(t)$. In this case, we retain the requirement that $U_c(\tau) = Q$, so that $U(\tau) = Q\tilde{U}(\tau)$.

3.2. Geometric treatment of decoherence: The error vector and control matrix

The error propagator $\tilde{U}(\tau)$, being an element of $SU(2)$, may be interpreted as a rotation of the qubit Bloch vector through some angle $2a(\tau)$, about an axis $\hat{\mathbf{a}}(\tau)$. Hence

$$\tilde{U}(\tau) = \exp\left[-i\mathbf{a}(\tau)\boldsymbol{\sigma}\right] \tag{7}$$

where $\mathbf{a}(\tau) \equiv a(\tau)\hat{\mathbf{a}}(\tau)$ is the real-valued 'error vector' with components $a_i(\tau)$, for $i \in \{x, y, z\}$, and magnitude $|a(\tau)| = \left(\mathbf{a}(\tau)\mathbf{a}^T(\tau)\right)^{1/2}$.

That a geometrical interpretation of the action of a propagator is possible in terms of a rotation of the Bloch vector is a consequence of the homomorphism that exists between $SU(2)$ and the group of three-dimensional rotation operators, $SO(3)$ [30]. In short, each propagator U and its physically equivalent negative $-U$, both elements of $SU(2)$, can be represented by a single rotation operator in $SO(3)$, in a way that preserves the group structure.

We may use this geometric interpretation to understand how the effect of arbitrary control modifies the evolution of the Bloch vector in time, in the presence of environmental noise. From Eqns. (5)-(7), we see that the error vector is determined by the toggling frame Hamiltonian $\tilde{H}_0(t)$, which itself derives from the action of the control propagator $U_c(t)$, an element of $SU(2)$, on $H_0(t)$. The homomorphism between $SU(2)$ and $SO(3)$ enables us to identify $U_c(t)$ with a three-dimensional 'control matrix' $\boldsymbol{R}(t) \in SO(3)$, following [29] but now explicitly incorporating time-dependent processes,

$$\begin{aligned}
\tilde{H}_0(t) &= \sum_{i=x,y,z} \beta_i(t) U_c^\dagger(t)\sigma_i U_c(t) && (8a)\\
&= \sum_{i,j=x,y,z} \beta_i(t) R_{ij}(t)\sigma_j && (8b)\\
&= \boldsymbol{\beta}(t)\boldsymbol{R}(t)\boldsymbol{\sigma} && (8c)
\end{aligned}$$

Using the orthogonality of the Pauli operators with respect to the Hilbert-Schmidt inner product, the elements of the control matrix are

$$R_{ij}(t) \equiv [\boldsymbol{R}(t)]_{ij} = \mathrm{Tr}\left(U_c^\dagger(t)\sigma_i U_c(t)\sigma_j\right)/2 \qquad (9)$$

for $i, j \in \{x, y, z\}$.

4. Calculating the Operational Fidelity

Our goal is thus effectively to characterize the argument of Eq. 7 using the formalism introduced above. In the specific case of dynamical error suppression, we go further and attempt to minimize this term. Accomplishing these goals will involve a series of analytic advances in how we calculate operational fidelity and capture the action of the control Hamiltonian. In the following sections we will describe our method in detail.

4.1. Approximating the error vector using the Magnus expansion

We seek an expression for the error vector $\mathbf{a}(\tau)$ by putting the solution to (6) in the simple exponential form (7). Due to the non-commuting nature of the operators affecting the quantum state during its evolution, this is not a straightforward task. However, at the cost of expressing the exponent as an infinite series, we can achieve the desired outcome using the Magnus expansion [34, 35, 36]. Specifically, given equation (6), we may write $\tilde{U}(\tau) = \exp\left[-i\Phi(\tau)\right]$, where

$$\Phi(\tau) = \sum_{\mu}^{\infty} \Phi_{\mu}(\tau) \tag{10a}$$

and

$$\Phi_1(\tau) = \int_0^{\tau} dt \tilde{H}_0(t) \tag{10b}$$

$$\Phi_2(\tau) = -\frac{i}{2}\int_0^{\tau} dt_1 \int_0^{t_1} dt_2 \left[\tilde{H}_0(t_1), \tilde{H}_0(t_2)\right] \tag{10c}$$

$$\begin{aligned}\Phi_3(\tau) = -\frac{1}{6}\int_0^{\tau} dt_1 \int_0^{t_1} dt_2 \int_0^{t_2} dt_3 \Big\{&\left[\tilde{H}_0(t_1), \left[\tilde{H}_0(t_2), \tilde{H}_0(t_3)\right]\right] \\ &+ \left[\tilde{H}_0(t_3), \left[\tilde{H}_0(t_2), \tilde{H}_0(t_1)\right]\right]\Big\}\end{aligned} \tag{10d}$$

with higher order terms involving increasingly complicated multiple integrals of nested commutators. Here the index μ indicates the order of the Magnus expansion.

We now exploit this general approach and the geometric interpretation of control to find expressions for the error vector. Returning to the control matrix introduced above, we compactly express Eq. (8c) as

$$\tilde{H}_0(t) = \sum_{i=x,y,z} \beta_i(t)\boldsymbol{r}_i(t)\boldsymbol{\sigma} \tag{11}$$

where we have written $\boldsymbol{R}(t) = (\boldsymbol{r}_x(t), \boldsymbol{r}_y(t), \boldsymbol{r}_z(t))^T$, with $\boldsymbol{r}_i(t) \equiv (R_{ix}(t), R_{iy}(t), R_{iz}(t))$ a row vector comprised of the i-th row of the control matrix. Substituting (11) into the above expressions for the Magnus expansion, and using the vector identity $[\mathbf{u}\boldsymbol{\sigma}, \mathbf{v}\boldsymbol{\sigma}] = 2i(\mathbf{u}\times\mathbf{v})\boldsymbol{\sigma}$, for $\mathbf{u}$, $\mathbf{v} \in \mathbb{R}^3$, we are able to write $\tilde{U}(\tau) = \exp\left[-i\sum_{\mu}^{\infty} \mathbf{a}_{\mu}(\tau)\boldsymbol{\sigma}\right]$, with the error vector in the form of an infinite series. The first three terms of this expansion are

$$\mathbf{a}_1(\tau) = \sum_{i=x,y,z} \int_0^{\tau} dt \beta_i(t)\mathbf{r}_i(t) \tag{12a}$$

$$\mathbf{a}_2(\tau) = \sum_{i,j=x,y,z} \int_0^{\tau} dt_1 \int_0^{t_1} dt_2 \beta_i(t_1)\beta_j(t_2)\tilde{\boldsymbol{r}}_{ij}(t_1, t_2) \tag{12b}$$

$$\mathbf{a}_3(\tau) = \frac{2}{3}\sum_{i,j,k=x,y,z} \int_0^{\tau} dt_1 \int_0^{t_1} dt_2 \int_0^{t_2} dt_3 \beta_i(t_1)\beta_j(t_2)\beta_k(t_3)\tilde{\boldsymbol{r}}_{ijk}(t_1, t_2, t_3) \tag{12c}$$

where we've introduced the vectors $\tilde{\boldsymbol{r}}_{ij}(t_1, t_2)) \equiv [\mathbf{r}_i(t_1) \times \mathbf{r}_j(t_2)]$ and $\tilde{\boldsymbol{r}}_{ijk}(t_1, t_2, t_3) \equiv [\mathbf{r}_i(t_1) \times [\mathbf{r}_j(t_2) \times \mathbf{r}_k(t_3)]] + [\mathbf{r}_k(t_3) \times [\mathbf{r}_j(t_2) \times \mathbf{r}_i(t_1)]]$. Generally, the n-th order term is an n-fold integral over the sum of all possible products of the form $\beta_{i_1}(t_1)\beta_{i_2}(t_2)...\beta_{i_n}(t_n)\tilde{\boldsymbol{r}}_{i_1 i_2 \ldots i_n}(t_1, t_2, ..., t_n)$, where the vector $\tilde{\boldsymbol{r}}_{i_1 i_2 \ldots i_n}(t_1, t_2, ..., t_n)$ is a sum of multiple vector cross products of rows of the control matrix $\boldsymbol{R}(t)$, evaluated at times $t_1, t_2, ..., t_n$.

4.2. Expressing the fidelity

One way of measuring how well a given propagator V_1 approximates a target operation V_2 is to take the Hilbert-Schmidt inner product $(V_2, V_1) \equiv \frac{1}{2}\,\mathrm{Tr}\,(V_2^\dagger V_1)$ which, by analogy with the usual inner product of state vectors, effectively measures the 'overlap' between the two operators. Taking the square modulus of the inner product of $U(\tau) = Q\tilde{U}(\tau)$ and Q, gives $\mathcal{F}(\tau) = \frac{1}{4}|\,\mathrm{Tr}(\tilde{U}(\tau))|^2$, an expression equivalent to the so-called single-qubit entanglement fidelity [37, 38]. This then serves to quantify the accuracy of a control operation, subject to a particular realization of the noise vector $\boldsymbol{\beta}(t)$. Experimentally, however, it is usually only the ensemble average of the entanglement fidelity

$$\mathcal{F}_{av}(\tau) \equiv \frac{1}{4}\langle|\,\mathrm{Tr}(\tilde{U}(\tau))|^2\rangle \tag{13}$$

taken over all realizations of the noise Hamiltonian (3), that is measured, and we therefore refer to (13) as determining the 'fidelity' of a particular control operation.

With the error propagator written in the form (7), and suppressing the explicit τ-dependence, one finds

$$\mathcal{F}_{av} = \frac{1}{2}\left[\langle\cos{(2a)}\rangle + 1\right] \tag{14}$$

so that, for each qubit in the ensemble, the fidelity is determined by the magnitude of the angle through which the noise causes the control operation to be *rotated* away from the target operation Q. Expanding the cosine term in a Taylor series we obtain

$$\mathcal{F}_{av} = \frac{1}{2}\left[1 + \sum_{m=0}^{\infty}(-1)^m\frac{2^{2m}}{(2m)!}\langle a^{2m}\rangle\right] \tag{15}$$

We proceed by evaluating the first nontrivial term ($m = 1$) in the expansion (the terms $\langle a^{2m}\rangle$, for $m > 1$ are obtainable similarly). Recalling that $a^2 = \mathbf{a}\mathbf{a}^T$, and using the Magnus expansion of the error vector $(12a)$, we may now write

$$\langle a^2\rangle = \sum_{\mu\nu}\langle\mathbf{a}_\mu\mathbf{a}_\nu^T\rangle = \left[\langle a_1^2\rangle + \langle a_2^2\rangle + ... + 2\left(\langle\mathbf{a}_1\mathbf{a}_2^T\rangle + \langle\mathbf{a}_1\mathbf{a}_3^T\rangle + \langle\mathbf{a}_2\mathbf{a}_3^T\rangle + ...\right)\right] \tag{16}$$

where $a_1^2 \equiv \mathbf{a}_1\mathbf{a}_1^T$, and μ, ν are indices over the order of the Magnus expansion. Finally, we arrive at the following series expansion for the fidelity

$$\mathcal{F}_{av} = 1 - \langle a_1^2\rangle - 2\langle\mathbf{a}_1\mathbf{a}_2^T\rangle - \left[\langle a_2^2\rangle + 2\langle\mathbf{a}_1\mathbf{a}_3^T\rangle - \frac{\langle a_1^4\rangle}{3}\right] + ... \tag{17}$$

with $a_2^2 \equiv \mathbf{a}_2\mathbf{a}_2^T$ and $a_1^4 \equiv (\mathbf{a}_1\mathbf{a}_1^T)^2$. The second term in (17)

$$\langle a_1^2\rangle = \sum_{i,j=x,y,z}\int_0^\tau dt_2\int_0^\tau dt_1\langle\beta_i(t_1)\beta_j(t_2)\rangle\boldsymbol{r}_i(t_1)\boldsymbol{r}_j^T(t_2) \tag{18a}$$

$$= \sum_{i,j,k=x,y,z}\int_0^\tau dt_2\int_0^\tau dt_1\langle\beta_i(t_1)\beta_j(t_2)\rangle R_{ik}(t_1)R_{jk}(t_2) \tag{18b}$$

contains all two-point noise cross-correlation functions $\langle\beta_i(t_1)\beta_j(t_2)\rangle$, for $i, j \in \{x, y, z\}$, while the third contains all those evaluated at three time points, and the terms in square brackets all involve four-point correlation functions (this is determined by the sum of subscript indices in a term as they indicate the expansion-order of the error vector in Eq. 12*a*-12*c*). For noise that is weak, the general trend will be for terms involving higher-order correlation functions to have less of an effect on the fidelity. Explicit forms for these terms, in the case that noise is purely dephasing (i.e. $H_0(t) = \beta_z(t)\sigma_z$), may be found in [39].

4.3. Moving to the Fourier domain

The form of the expressions contributing to the fidelity above may be calculated explicitly, but rely on time-domain correlation and cross-correlation functions and convolution with the multidimensional control matrix. Relying on the properties of the Fourier transform it is experimentally convenient to write these terms in the frequency domain. Generally, we can define the Fourier transform $\mathcal{S}_{i_1...i_n}(\omega_1, ..., \omega_n)$ of an n-point cross-correlation function via

$$\langle\beta_{i_1}(t_1)\beta_{i_2}(t_2)...\beta_{i_n}(t_n)\rangle \equiv \frac{1}{(2\pi)^n}\int d\omega_1...\int d\omega_n \mathcal{S}_{i_1...i_n}(\omega_1, ..., \omega_n)e^{i(\omega_1 t_1+...+\omega_n t_n)} \tag{19}$$

The fidelity (17) can then be rewritten as

$$\mathcal{F}_{av} = 1 - \sum_{n=2}^{\infty}\left\{\frac{1}{(2\pi)^n}\sum_{i_1...i_n}\int d\omega_1...\int d\omega_n \mathcal{S}_{i_1...i_n}(\omega_1, ..., \omega_n)\mathcal{R}i_1...i_n(\omega_1, ..., \omega_n)\right\} \tag{20}$$

where $\mathcal{R}_{i_1...i_n}(\omega_1, ..., \omega_n)$ is determined solely by the control matrix.

For noise that is sufficiently weak, the $n = 2$ term in (20) will be the dominant contributor to fidelity loss in the short term, i.e. $\mathcal{F}_{av} \approx 1 - \langle a_1^2\rangle$. If the noise is also *wide sense stationary* then the two-point cross-correlation functions depend only on the time difference $t_2 - t_1$, so that

$$\langle\beta_i(t_1)\beta_j(t_2)\rangle = \frac{1}{2\pi}\int_{-\infty}^{\infty} d\omega S_{ij}(\omega)e^{i\omega(t_2-t_1)} \tag{21}$$

where $S_{ij}(\omega)$ is the cross-power spectral density between the random variables $\beta_i(t)$ and $\beta_j(t)$. We then have

$$\langle a_1^2\rangle = \frac{1}{2\pi}\sum_{i,j,k=x,y,z}\int_{-\infty}^{\infty}\frac{d\omega}{\omega^2}S_{ij}(\omega)R_{jk}(\omega)R_{ik}^*(\omega) \tag{22}$$

where

$$R_{ij}(\omega) \equiv -i\omega\int_0^{\tau} dt R_{ij}(t)e^{i\omega t} \tag{23}$$

are the elements of the control matrix in the frequency domain (again we suppress the explicit dependence on the total time τ). The form of (22) is reminiscent of the filter function introduced in previous literature on dynamical error suppression, to which we will return later. Thus, in the weak noise regime, it is possible to understand the fidelity of a qubit's unitary evolution in terms of spectral properties of the noise and the control [9, 18]. In the next section we will show how the control matrix may be evaluated for the paradigmatic case of a piecewise constant control sequence. In doing so, we explicitly demonstrate the connection between our generalized approach and the well known filter-function formalism.

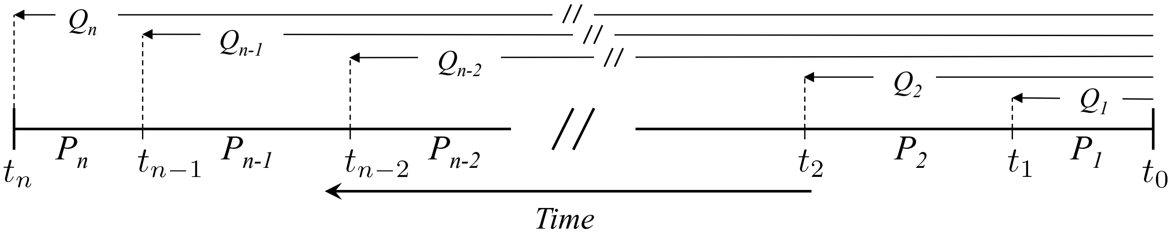

Figure 2. Explanatory diagram for a piecewise-defined control sequence. During each interval $[t_{l-1}, t_l]$, a control operation P_l is executed. The operators Q_l are the control propagator evaluated at the start of the l-th pulse, for $l = 1, 2, .., n$.

5. Evaluating the control matrix

In general, for arbitrary continuous-time modulation of $H_c(t)$, the control matrix can be evaluated only approximately. However, using the simplifying assumption of piecewise-constant control it becomes possible to find an exact analytic form for the control matrix. This model can be applied to dynamical decoupling sequences (π-pulses separated by free-evolution periods, ultimately implementing the identity operation I), as well as a variety of nontrivial control operations such as piecewise-defined dynamically corrected gates and composite pulses [40, 41].

5.1. Universal noise

For a sequence of n consecutive unitary control operations $P_1, ..., P_n$, we divide the total sequence time τ into n corresponding time bins $[t_{l-1}, t_l]$, such that $P_l = U_c(t_l, t_{l-1})$, for $l \in \{1, 2, ..., n\}$, with $t_n \equiv \tau$ and $t_0 \equiv 0$ (Figure 2). Letting $P_0 \equiv I$, and defining the cumulative operators $Q_l \equiv P_l P_{l-1} ... P_0$ and $Q \equiv Q_n$, equation (9) becomes

$$R_{ij}(t) = \frac{1}{2} \sum_{l=1}^{n} G^{(l)}(t) \operatorname{Tr} \left(Q_{l-1}^{\dagger} U_c^{\dagger}(t, t_{l-1}) \sigma_i U_c(t, t_{l-1}) Q_{l-1} \sigma_j \right) \tag{24}$$

where the function $G^{(l)}(t) \equiv \Theta[t - t_{l-1}] - \Theta[t - t_l]$ has unit value within the l-th time bin and is zero elsewhere. Equation (24) can be rewritten in terms of the control matrices $\boldsymbol{R}^{P_l}(t - t_{l-1})$ for each of the n operations P_l in the sequence, defined relative to the pulses start times t_{l-1}, by letting

$$U_c^{\dagger}(t, t_{l-1}) \sigma_i U_c(t, t_{l-1}) = \sum_{k=x,y,z} R_{ik}^{P_l}(t - t_{l-1}) \sigma_k \tag{25}$$

for $i \in \{x, y, z\}$. Again, the components of $\boldsymbol{R}^{P_l}(t - t_{l-1})$ are found using the Hilbert-Schmidt inner product

$$R_{ij}^{P_l}(t - t_{l-1}) \equiv [\boldsymbol{R}^{P_l}(t - t_{l-1})]_{ij} = \frac{1}{2} \operatorname{Tr} \left(U_c^{\dagger}(t, t_{l-1}) \sigma_i U_c(t, t_{l-1}) \sigma_j \right) \tag{26}$$

for $i, j \in \{x, y, z\}$. Substituting (25) into (24), and using the linearity of the trace operation, we find that we can write the control matrix for the pulse sequence in the compact form

$$\boldsymbol{R}(t) = \sum_{l=1}^{n} G^{(l)}(t)\boldsymbol{R}^{P_l}(t - t_{l-1})\boldsymbol{\Lambda}^{(l)} \tag{27}$$

where the matrix $\boldsymbol{\Lambda}^{(l)}$ has components

$$\Lambda_{ij}^{(l)} \equiv \frac{1}{2}\operatorname{Tr}\left(Q_{l-1}^{\dagger}\sigma_i Q_{l-1}\sigma_j\right) \tag{28}$$

for $i, j \in \{x, y, z\}$. Using (23) to switch to the frequency domain, we have

$$\boldsymbol{R}(\omega) = \sum_{l=1}^{n} e^{i\omega t_{l-1}}\boldsymbol{R}^{P_l}(\omega)\boldsymbol{\Lambda}^{(l)} \tag{29a}$$

with

$$\boldsymbol{R}^{P_l}(\omega) \equiv -i\omega \int_0^{t_l - t_{l-1}} dt e^{i\omega t}\boldsymbol{R}^{P_l}(t) \tag{29b}$$

With the above expressions and a knowledge of the statistical properties of the noise, using the results of Sec. 4 we can find an approximate value for the fidelity of an arbitrary piecewise-defined control sequence in a universal weak noise environment. Despite the proliferation of terms in these analytic expressions, this approach is straightforward to implement by hand or through numerics. Ultimately the computational efficiency of calculating the control matrix and spectral overlap integrals far exceeds that of brute-force numerical simulations of the evolution of the Bloch vector [39].

5.2. Pure Dephasing

In many of the physical systems with the potential for use in nascent quantum information technologies, the characteristic single-qubit dephasing time T_2 is considerably smaller than the relaxation time T_1, and governed by different physical processes. It is important, therefore, that we understand the effects of purely dephasing noise on single-qubit control. To this end, we consider a model system in which the noise vector $\boldsymbol{\beta}(t)$ has only a z-component and the noise Hamiltonian (3) reduces to

$$H_0(t) = \beta_z(t)\sigma_z \tag{30}$$

Only the third row of the control matrix, $\boldsymbol{r}_z(t) \equiv (R_{zx}(t), R_{zy}(t), R_{zz}(t))$, is required to calculate the fidelity. So, for the sake of notational simplicity, we drop the z subscript from this point on and refer to $\boldsymbol{r}(t) \equiv \boldsymbol{r}_z(t)$ simply as the ‘control vector’, with components $r_i(t) \equiv R_{zi}(t)$, for $i \in \{x, y, z\}$.

With the dephasing Hamiltonian (30), the lowest-order contribution (22) to the fidelity (17) simplifies to

$$\langle a_1^2 \rangle = \frac{1}{2\pi}\int_{-\infty}^{\infty}\frac{d\omega}{\omega^2}S(\omega)F_1(\omega) \tag{31}$$

where $S(\omega) \equiv S_{zz}(\omega)$, and the first order ‘filter function’ $F_1(\omega)$ is simply the square magnitude of the frequency domain control vector

$$F_1(\omega) \equiv |\boldsymbol{r}(\omega)|^2 = \sum_{i=x,y,z} |r_i(\omega)|^2 \tag{32}$$

If we further assume that the noise is Gaussian, with a mean value of zero, then all correlation functions $\langle \beta_z(t_1)...\beta_z(t_n)\rangle$ for which n is odd are equal to zero. The Gaussian moment theorem also allows us to write all remaining higher-order correlations in terms of only the simplest two-point correlation function. In the frequency domain, the statistical properties of the noise are then captured entirely by the power spectral density $S(\omega)$, and the fidelity (17) can be written as the infinite sum [39]

$$\mathcal{F}_{av} = 1 - \left[\frac{1}{2\pi}\int_{-\infty}^{\infty}\frac{d\omega}{\omega^2}S(\omega)F_1(\omega) \right. \\ \left. + \frac{1}{(2\pi)^2}\int_{-\infty}^{\infty}\frac{d\omega}{\omega^2}S(\omega)\int_{-\infty}^{\infty}\frac{d\omega'}{\omega'^2}S(\omega')F_2(\omega,\omega') + ...\right] \qquad (33)$$

Here, the effect of the control on the qubit fidelity is described by the functions F_p, for $p = 1, 2, ...$, which depend only on the control vector $\boldsymbol{r}$. The complexity of the filter functions increases rapidly with increasing order. However, $F_1(\omega)$ can be quite simple in form and reasonably straightforward to calculate. In the weak noise regime we ignore the higher order terms in (33) and write

$$\mathcal{F}_{av}(\tau) \simeq \frac{1}{2}\left\{1 + \exp\left[-\chi(\tau)\right]\right\} \qquad (34a)$$

where the rate of fidelity decay is given by

$$\chi(\tau) \equiv \langle a_1^2\rangle = \frac{1}{\pi}\int_0^{\infty}\frac{d\omega}{\omega^2}S(\omega)F_1(\omega) \qquad (34b)$$

Thus, the decay rate is determined by a simple overlap integral between the power spectrum of the noise and a "filter function" representing the control in the Fourier domain. This result is similar to the familiar expression for the coherence of a dynamical decoupling sequence in the case of unbounded controls [18] (see also Sec. 6). The difference here being that the filter function F_1 captures only the lowest order nontrivial effect of the control on the fidelity in a dephasing environment, rather than providing an exact solution in the bang-bang limit.

For a piecewise-defined sequence, Eq. (24) reduces to the following expression for the components of the control vector

$$r_i(t) = \frac{1}{2}\sum_{l=1}^{n} G^{(l)}(t)\,\mathrm{Tr}\left(Q_{l-1}^{\dagger}U_c^{\dagger}(t,t_{l-1})\sigma_z U_c(t,t_{l-1})Q_{l-1}\sigma_i\right) \qquad (35)$$

Equations (29a) and (29b) become

$$\boldsymbol{r}(\omega) = \sum_{l=1}^{n} e^{i\omega t_{l-1}}\boldsymbol{r}^{P_l}(\omega)\boldsymbol{\Lambda}^{(l)} \qquad (36a)$$

$$\boldsymbol{r}^{P_l}(\omega) \equiv -i\omega\int_0^{t_l - t_{l-1}} dt e^{i\omega t}\boldsymbol{r}^{P_l}(t) \qquad (36b)$$

respectively, where the components of the l-th pulse control vector are

$$r_j^{P_l}(t - t_{l-1}) = \frac{1}{2}\,\mathrm{Tr}\left(U_c^{\dagger}(t,t_{l-1})\sigma_z U_c(t,t_{l-1})\sigma_j\right) \qquad (37)$$

for $j \in \{x, y, z\}$.

If we assume that during each of the n time bins comprising the sequence the applied control effects a steady rotation of the qubit Bloch vector through an angle θ_l, about an axis $\hat{\boldsymbol{n}}_l = \cos(\phi_l)\hat{x} + \sin(\phi_l)\hat{y}$ in the xy-plane, then for $t \in [t_{l-1}, t_l]$

$$U_c(t, t_{l-1}) = \exp\left[\frac{-i}{2}\Omega_l\,(t - t_{l-1})\,\sigma_{\phi_l}\right] \tag{38}$$

where $\Omega_l \equiv \theta_l/(t_l - t_{l-1})$ is the rotation rate and $\sigma_{\phi_l} \equiv \cos(\phi_l)\sigma_x + \sin(\phi_l)\sigma_y$. From (37) and (36$b$) we can show that the frequency domain control vector for the l-th operation has components

$$r_j^{P_l}(\omega) = \frac{\omega}{\omega^2 - \Omega_l^2}\left\{\delta_{zj}\left[i\Omega_l g_l(\omega) - \omega f_l(\omega)\right] + \left[\Omega_l f_l(\omega) - i\omega g_l(\omega)\right]\mathrm{Tr}\left(\sigma_{\phi_l}\sigma_z\sigma_j\right)\right\} \tag{39}$$

where $f_l(\omega) \equiv e^{i\omega(t_l - t_{l-1})}\cos(\theta_l) - 1$ and $g_l(\omega) \equiv e^{i\omega(t_l - t_{l-1})}\sin(\theta_l)$. Although (39) has been derived assuming rotations take place about axes in the xy-plane only, periods of free evolution (no rotation) and z-axis rotations are easily accounted for by setting $\theta_l = 0$ and $\Omega_l = 0$ in (39), whenever one of these operations occurs in the sequence. This is possible simply because, for dephasing noise, both of these operations commute with the noise operator.

With these tools, the process for finding the operational fidelity of an arbitrary piecewise-constant control sequence in the presence of dephasing noise may be summarized as follows:

(i) Calculate the matrix given by Eq. (28) for each step in the chain of control operations

(ii) Substitute the above result as well as Eq. (39) into Eq. (36a)

(iii) Repeat for all time steps $l \in [1, n]$ to find the control vector in the Fourier domain

(iv) Find the first-order filter function from Eq. (32)

(v) Use Eqs. (34a) and (34b) to calculate approximate expression for the fidelity valid for weak dephasing noise.

In the next section we employ this approach to treat the important problem of studying pulse imperfections on the performance of dynamical decoupling sequences used in quantum memory.

6. Example: Pulse effects in dynamical decoupling

The aim of dynamical error suppression protocols, in the language described above, is to perform a desired control operation Q without significant error by constructing $H_c(t)$ such that it *modifies* the action of the noise Hamiltonian to affect $\tilde{U}(\tau) \to I$, the identity operation. In particular, a large body of literature has been devoted to the study of dynamical decoupling (DD) sequences. These are control protocols aimed at implementing the identity operator ($Q = I$) and thus preserving the initial state of the qubit; decoherence is effectively time-reversed by the action of the control sequence.

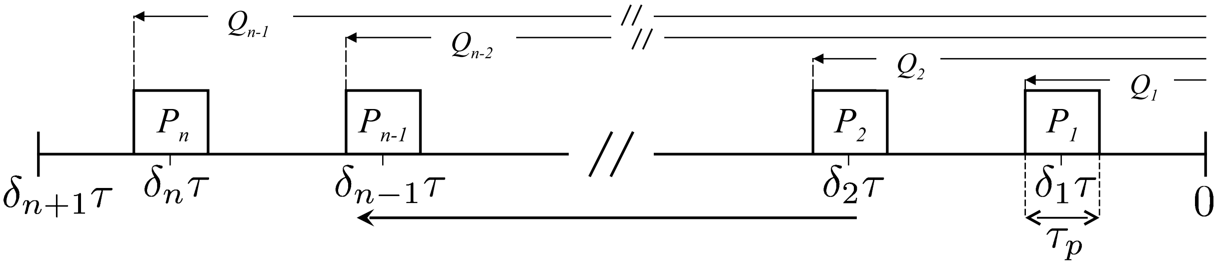

Figure 3. Dynamical decoupling sequence for n identical pulses, each of width τ_P, centered at times $\delta_l\tau$, for $l = 1, 2, .., n$

In the limit of instantaneous control pulses and in the particular case of a semi-classical dephasing environment (or equivalently a spin-boson model), it has been shown that it is possible to write the qubit coherence at the end of an arbitrary DD sequence, given preparation of the system in a superposition of eigenstates of σ_z, as $W = e^{-\chi(\tau)}$ [42, 21]. In this expression, the effect of both the noisy dephasing environment and the control modulation are captured in the overlap integral

$$\chi(\tau) = \frac{1}{\pi}\int_0^\infty \frac{d\omega}{\omega^2} S(\omega)F(\omega)d\omega. \tag{40}$$

The terms in this integral include the statistical properties of the noise in the Fourier domain through the noise power spectrum $S(\omega)$, and the action of the control sequence through the filter function, $F(\omega)$. This expression is formally identical to equation (34*b*) above, with the exception that, because the control pulses are assumed to be unbounded in strength with vanishing duration (the so-called "bang-bang" approximation), the filter function in (40) is exact. The bang-bang approximation is, however, unphysical and has been shown in experiment to neglect important contributions to the net error arising from the π_X control operations with nonzero width τ_p, that constitute the sequence (see Fig. 3).

In this section we will apply the techniques we have developed to evaluate the fidelity of dynamical decoupling sequences when considering physical constraints - such as the incorporation of realistic control pulses. In order to understand how well a given DD sequence suppresses error we must efficiently evaluate the filter functions, accounting for the various errors that arise when performing realistic control pulses in a dephasing environment. We adapt the results presented in section (5) for an *arbitrary* control sequence to the specific case of dynamical decoupling with bounded pulses of finite width, and show how the form of the pulses may be analytically separated from the applied pulse sequence.

6.1. Separating pulses from the pulse sequence

DD sequences can differ in both the spacing and form of the pulses in time. To find optimal error-suppressing sequences for a given environment or physical system, either of these variables may be changed independently of the other, and these differences must be easily separated in an analytical framework. We are therefore motivated to express the sequence control vector $\mathbf{r}(\omega)$ in terms that can be separated into those dependent only on pulse *location* (δ_l) and those dependent on pulse *type* (expressed in terms of the *pulse* control vector $\mathbf{r}^P(\omega)$).

As in section (5), we start with a piecewise constant sequence of n pulses, however, here we exploit the simplicity of the actual control Hamiltonian to streamline the process. Explicitly, we assume that the pulses are identical, each of width τ_p and executing a net π-rotation of the qubit Bloch vector about the x axis, i.e., $P_l = \sigma_x$, for $l \in \{1, 2, ..., n\}$. In addition, both before and after each pulse we include a period of free evolution (i.e., no control operation), so that immediately following the l-th pulse, we have $Q_l = P_l I P_{l-1} I ... I P_0$. In effect, we have two interleaved subsequences: a subsequence of n disjoint control pulses and a subsequence of $n+1$ disjoint free evolution periods. Within the total sequence time τ (including both control pulses and free evolution periods), the center of the l-th pulse occurs at a time $\delta_l \tau$, where $0 \leq \delta_l \leq 1$ and $\delta_{n+1} = 1$ (see Figure 3).

Due to the cumulative nature of the control propagator, the pulse and free evolution subsequences are not independent. In particular, the operator Q_l results in change in sign of both the pulse and free evolution control vectors at the conclusion of each pulse. From (36a) and (39) (with $\Omega_l = 0$), the control vector for a sequence of free evolution periods extending over the disjoint time intervals $[0, \delta_1\tau - \tau_P/2], [\delta_1\tau + \tau_P/2, \delta_2\tau - \tau_P/2], ..., [\delta_n\tau + \tau_P/2, \tau]$, with a change of sign during each successive interval, reduces to a single component

$$r_z(\omega) = 1 - e^{i\omega\tau} + 2\cos(\omega\tau_p/2) \sum_{l=1}^{n} (-1)^l e^{i\omega\delta_l\tau}. \tag{41}$$

The same result was derived previously by assuming finite-width pulses during which noise was ignored [22, 21]. In the bang-bang limit of infinitely narrow pulses ($\tau_p \to 0$) we have the standard result (for even n)

$$r(\omega) = 1 - e^{i\omega\tau} + 2 \sum_{l=1}^{n} (-1)^l e^{i\omega\delta_l\tau}. \tag{42}$$

with $F(\omega) = |r_z(\omega)|^2$.

Incorporating noise during pulses, arbitrary pulse forms, and arbitrary DD sequences has heretofore been impossible by simple analytic methods. By taking account of the terms dependent on $\mathbf{r}^P$, the accumulation of error during the control pulses and the effects of pulse shape on this error can be calculated for arbitrary decoupling sequences. Using a method similar to that above, we can derive the control vector for the subsequence of disjoint pulses – with arbitrary form – alone. Adding this to (41) gives us the control vector for a total decoupling sequence, which now has the two nonzero components

$$r_z(\omega) = 1 - e^{i\omega\tau} + \left[2\cos(\omega\tau_p/2) - e^{-i\omega\tau_p/2} r_z^P(\omega)\right] \sum_{l=1}^{n} (-1)^l e^{i\omega\delta_l\tau} \tag{43a}$$

$$r_y(\omega) = -e^{-i\omega\tau_p/2} r_y^P(\omega) \sum_{l=1}^{n} (-1)^l e^{i\omega\delta_l\tau} \tag{43b}$$

These expressions capture modification of dephasing dynamics due to the duration and form of the pulses as well as depolarization effects occurring due to pulse-errors derived from a fluctuating detuning from resonance (i.e. the impact of dephasing noise).

We will move forward using these expressions in order to treat experimentally relevant cases of DD incorporating various pulse forms including error-suppressing dynamically corrected gates.

6.2. Pulse Forms: Standard π_X-Pulses and Dynamically Corrected Gates

For a DD sequence we are interested in physical control operations that implement a logical NOT gate. The simplest approach is to employ "primitive" π_X-pulses, implemented by applying the ideal control Hamiltonian $H_c = \Omega\sigma_x/2$ over a time interval $[0, \tau_\pi]$, where $\Omega \equiv \pi/\tau_\pi$. This induces a simple rotation of the Bloch vector through an angle of π radians about the x-axis. With this geometrical picture it is possible to understand the accumulation of error during a pulse using the method we have described in detail above. In the presence of time-varying dephasing noise, the bare gate is modified by an error term that, to first order, results in a small additional rotation about an axis that has both y and z-components. From equations (36a) and (39) we find that the two corresponding components of control vector are

$$r_z^P \equiv r_z^{(Prim)}(\omega) = \frac{\omega^2}{\omega^2 - \Omega^2}\left(e^{i\omega\tau_\pi} + 1\right) \tag{44a}$$

$$r_y^P \equiv r_y^{(Prim)}(\omega) = \frac{i\omega\Omega}{\omega^2 - \Omega^2}\left(e^{i\omega\tau_\pi} + 1\right) \tag{44b}$$

It is interesting to note the correspondence between the prefactors here and those arising in a master-equation treatment of a driven quantum system in the presence of dissipation [43].

Moving beyond the standard π_X-pulse of finite duration, we consider a gate that has been designed to provide robustness in the presence of random gate errors - the dynamically corrected gate. In previous work we demonstrated how such gates provide enhanced resistance to error in the presence of time-varying dephasing noise [39]. Here we include expressions for a dynamically corrected logical NOT gate consisting of three successive π_X pulses, the second of which is executed at a rotation rate $\Omega/2$, half that of the other two [44]. The control Hamiltonian for this sequence is

$$H_c(t) = \begin{cases} \Omega\sigma_x/2 & 0 \le t < \tau_\pi \\ \Omega\sigma_x/4 & \tau_\pi \le t < 3\tau_\pi \\ \Omega\sigma_x/2 & 3\tau_\pi \le t \le 4\tau_\pi \end{cases} \tag{45}$$

In the case of dephasing noise, the control vector again has two components:

$$r_z^P \equiv r_z^{(DCG)}(\omega) = \omega^2 \left[\frac{p_1(\omega)}{\omega^2 - \Omega^2} - \frac{p_2(\omega)}{\omega^2 - (\Omega/2)^2}\right] \tag{46a}$$

$$r_y^P \equiv r_y^{(DCG)}(\omega) = i\omega\Omega\left[\frac{p_1(\omega)}{\omega^2-\Omega^2} - \frac{p_2(\omega)/2}{\omega^2-(\Omega/2)^2}\right] \tag{46b}$$

where $p_1(\omega) \equiv e^{4i\omega\tau_\pi} + e^{3i\omega\tau_\pi} + e^{i\omega\tau_\pi} + 1$ and $p_2(\omega) \equiv e^{3i\omega\tau_\pi} + e^{i\omega\tau_\pi}$.

6.3. Interpreting the filter function

The inset to Figure 4a shows the filter functions, $F_1(\omega) \equiv |r_y^P(\omega)|^2 + |r_z^P(\omega)|^2$, for the primitive and dynamically corrected logical NOT operations described above, as a function of the angular frequency in units of τ_π^{-1}. The filter function grows with ω, capturing the low-frequency "filtering" performance of DD sequences. Beyond a certain frequency $F_1(\omega) \to 1$, above which noise is passed unimpeded. This corresponds to the physical observation that fluctuations fast relative to the shortest interpulse period cannot be effectively suppressed by dynamical decoupling.

The filter function's behavior near zero frequency captures the leading-order error susceptibility. We may express $F_1(\omega) \propto (\omega\tau_\pi)^{2(\alpha+1)}$ as $\omega\tau_\pi \to 0$, then α is the order of error suppression for the sequence [45]. Using these expressions, an examination of Fig. 4 reveals that the relative performance of the primitive and dynamically corrected gates is captured in the slope of the filter function as plotted on a log-log scale [20]; higher slope corresponds to a higher order of error suppression (for noise near zero frequency) due to the multiplicative nature of the filter function in (34*b*). In a filter-design framework we may refer to this slope as a filter rolloff in the stopband, using the relation that the rolloff is $6(\alpha+1)$ dB/octave. At low frequencies the primitive π_X-pulse filter function is approximately quadratic, i.e. $F(\omega) \propto (\omega\tau_\pi)^2$, resulting in $\alpha = 0$ - the same as for free evolution. This is not a surprising result, since there is no error suppression built into the primitive gate. By contrast the DCG filter function scales as $F(\omega) \propto (\omega\tau_\pi)^4$, giving $\alpha = 1$, as expected for a construction designed to suppress error to first order.

6.4. The full filter functions: DD + DCG

We now combine the control vectors derived for the pulses themselves with those obtained for the generic DD sequences, considering three paradigmatic cases: (1) bang-bang decoupling, (2) standard pulses with nonzero τ_p, (3) DCGs. This is accomplished by calculating $\boldsymbol{r}^P$ and inserting the relevant Cartesian components into Eqs. 43a and 43b for the full DD sequence. This study reveals how it is possible to evaluate complex perturbations to quantum control protocols in a straightforward manner using our method.

We compare the error-suppressing performance of CP and UDD sequences as illustrative examples, accounting for each of the cases outlined above. The CP sequence, first proposed by Carr and Purcell in the context of NMR [46], is a straightforward extension of the original Hahn spin echo [47]. In an n-pulse CP sequence, the l-th pulse has the fractional location $\delta_l = (l - 1/2)/n$. The bang-bang limit CP filter function for $n = 6$ is shown as a black line in Figure 4a) for $n = 6$. It exhibits an order of error suppression of $\alpha = 2$, as do all CP sequences with $n \geq 2$, giving a roll-off of 18 dB/octave. This is a limiting case in which pulse effects are entirely ignored.

If we now take into account the width of the pulses by assuming that they take the form of primitive NOT gates of width τ_p, as described above, then the components of the pulse control vector $\boldsymbol{r}^P(\omega)$ are given by equations $(44a)$ and $(44b)$. The resulting filter functions, indicated by the blue lines in Figure 4a) show a reduced order of error suppression $\alpha = 2 \rightarrow 1$, with a corresponding reduction of the filter rolloff to 12dB/octave. As the pulse width grows as a fraction of the entire sequence, the relative importance of the pulses grows, as expected. This is manifested as an expansion of the range over which the modification to the filter-function due to pulse effects dominates the bang-bang filter function.

Despite the reduction in the order of error suppression, there is still noise cancelation, regardless of the pulse width, since the sequence is in essence an Eulerian dynamical decoupling (EDD) sequence [48]. Replacing the primitive pulses with dynamically corrected composite gates and the components of the pulse control vector with $(46a)$ and $(46b)$, we almost completely restore the original 18dB/octave roll-off for the CP sequences (Figure 4a). These filter functions lie approximately beneath the bang-bang filter function in this figure. This observation confirms that the DCG provides one order of error cancellation during the applied pulses. In essence, the deleterious effect of error accumulation during nonzero-duration control pulses can be mitigated by appropriate choice of a DCG.

Studying UDD is more instructive because the n-pulse UDD sequence, with relative

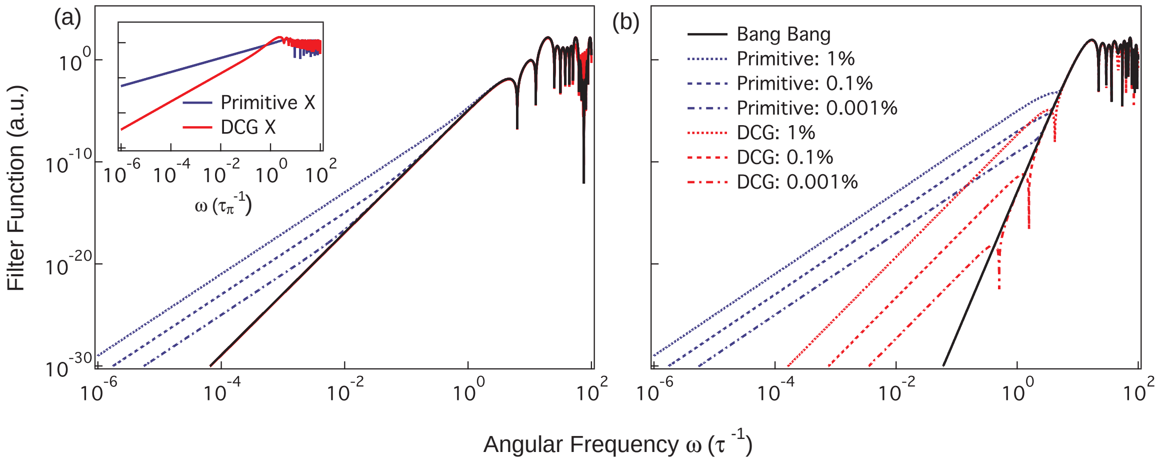

Figure 4. First order filter functions as a function of dimensionless frequency. The inset of a) compares filter functions for primitive (blue) and dynamically corrected (red) NOT gates while the main plot shows filter functions for a 6 pulse CP sequence. The results for primitive NOT pulses are shown in blue, while those for dynamically corrected pulses are shown in red. Plot b) shows the same set of results for the 6 pulse UDD sequence. Black lines represent filter functions for sequences in the bang-bang limit

pulse locations given by $\delta_l = \sin^2[\pi l/(2n+2)]$, ensures that (in the bang bang limit) the first n-derivatives of $r_z(\omega)$ vanish at $\omega = 0$ [18, 42], giving an order of error suppression that increases linearly with n. The effects of pulse width and shape are therefore relatively more dramatic due to the high order of error suppression for, e.g. $n = 6$, as shown in Fig. 4b). For sufficiently long pulses we see that the general benefits derived from the use of a UDD sequence can largely be destroyed as the error-susceptibility of the pulses dominates the suppression provided by the pulse timing. Again, we observe that the reduction in the order of error suppression arising from addition of nonzero-duration π_X-pulses can be partially offset by use of a DCG. However, the fact that by design, the DCG used here only provides first-order error suppression, reduces our ability to recover the original order of error suppression provided by a UDD sequence with large n.

Nonetheless, these results indicate that judicious choice of DCG or other compensating pulse protocols within DD sequences provides a path to mitigate the effects of pulse errors in DD sequences. This is especially important in long-storage settings where large pulse numbers may be employed in order to effectively suppress dephasing errors [49]. These observations represent an important validation of our method, and show that it provides a straightforward approach to account for a variety of pulse-duration, modulation, and shape effects.

7. Conclusion

Understanding, predicting, and mitigating decoherence remain significant challenges for the development of quantum technologies. In particular, in order to effectively develop novel quantum control protocols that suppress error or evaluate the performance of a complex quantum error correction procedure, we require methods permitting a system designer to estimate error probabilities using real inputs about the environment. This capability is vital as the quantum science community moves from proof-of-principle concepts towards engineering of real quantum coherent technologies where rigid performance bounds are required.

In this paper, we have presented a novel method for determining the fidelity of arbitrary quantum control operations in a universal time-dependent noise environment. Building on past work employing spectral overlap functions, our method provides a straightforward, easily automated approach to producing analytic functions capturing the effect of the control in the Fourier domain – generalized filter functions. Using these we are able to evaluate control fidelities to arbitrary order, for arbitrary time-dependent control operations in terms of experimentally relevant characteristics of the noise. While the error model we study is constrained to ignore, e.g., leakage errors from the qubit subspace or system-bath entanglement, the selected semiclassical model of universal, Non-Markovian, time-varying noise is far more realistic than earlier approximations based on uncorrelated errors.

We have exploited the capabilities provided by this technique to address the key challenge of accounting for nonidealities in control operations used to implement error-suppressing dynamical decoupling sequences. By generating filter functions incorporating pulse errors and even the effect of complex intrapulse modulation schemes in a single compact formalism, we have provided a simple, physically intuitive means to evaluate sequence performance and inform the development of new dynamical error suppression protocols.

Our approach permits an experimentalist or system designer to analytically study the efficacy and error-susceptibility of customized control protocols involving complex temporal modulation schemes (e.g. control-field phase and amplitude). For instance, it is possible to accurately account for error accumulation due to *control imperfections* arising from realistic constraints such as pulse overshoot, bandwidth limitations, or simple noise in the control field itself. Further, for quantum information one may consider applying this approach at an algorithmic level, permitting "echo" type effects to be exploited in minimizing the error not just of a single operation, but of a complex chain in a computation. With validation for the utility of our method from our study of dynamical decoupling, we believe that this approach will prove invaluable for future experiments in which it is vital to accurately and efficiently estimate the effects of real experimental noise on the achievable fidelity of control operation.

Acknowledgements: The authors thank A.C Doherty, K. Khodjasteh, and L. Viola for useful discussions. This work partially supported by the US Army Research Office under Contract Number W911NF-11-1-0068, the Australian Research Council Centre of Excellence for Engineered Quantum Systems CE110001013, and the Office of the Director of National Intelligence (ODNI), Intelligence Advanced Research Projects Activity (IARPA), through the Army Research Office. All statements of fact, opinion or conclusions contained herein are those of the authors and should not be construed as representing the official views or policies of IARPA, the ODNI, or the U.S. Government.

References

[1] Tarn T J, Huang G and Clark J W 1980 *Math. Modeling.* **1** 109–121
[2] Huang G M, Tarn T J and Clark J W 1983 *J. Math. Phys.* **24** 2608
[3] Clark J W, Lucarelli D G and Tarn T J 2003 *Int. J. .Mod. Phys. B* **17** 5397
[4] Bouten L, Handel R V and James M R 2007 *SIAM J. Control Optim.* **46** 2199–2241
[5] Nurdin H I, James M R and Petersen I R 2009 *Automatica* **45** 1837–1846
[6] Wiseman H M and Milburn G J 2010 *Quantum Measurement and Control* (Cambridge: Cambridge University Press)
[7] D'Alessandro D 2007 *Introduction to Quantum Control and Dynamics* (Boca Raton: Taylor & Francis)
[8] Nielsen M and Chuang I 2010 *Quantum Computation and Quantum Information: 10th Anniversary Edition* (Cambridge: Cambridge University Press)
[9] Kofman A G and Kurizki G 2001 *Phys. Rev. Lett.* **87** 270405
[10] Kofman A G and Kurizki G 2004 *Phys. Rev. Lett.* **93** 130406
[11] Ban M 1998 *Journal of Modern Optics* **45** 2315
[12] Viola L and Lloyd S 1998 *Phys. Rev.* A **58** 2733

[13] Viola L, Knill E and Lloyd S 1999 *Phys. Rev. Lett.* **82** 2417

[14] Zanardi P 1999 *Phys. Lett.* A **258** 77

[15] Vitali D and Tombesi P 1999 *Phys. Rev.* A **59** 4178

[16] Khodjasteh K and Viola L 2009 *Phys. Rev. Lett.* **102** 080501

[17] Khodjasteh K and Viola L 2009 *Phys. Rev.* A **80** 032314

[18] Uhrig G S 2007 *Phys. Rev. Lett.* **98** 100504

[19] Cywiński L, Lutchyn R M, Nave C P and Das Sarma S 2008 *Phys. Rev. B* **77** 174509

[20] Biercuk M J, Doherty A C and Uys H 2011 *J. Phys. B: At. Mol. Opt. Phys.* **44** 154002

[21] Biercuk M J, Uys H, VanDevender A P, Shiga N, Itano W M and Bollinger J J 2009 *Phys. Rev. A* **79** 062324

[22] Biercuk M J, Uys H, VanDevender A P, Shiga N, Itano W M and Bollinger J J 2009 *Nature* **458** 996

[23] de Lange G, Wang Z H, Rist D, Dobrovitski V V and Hanson R 2010 *Science* **330** 60

[24] Bluhm H, Foletti S, Neder I, Rudner M, Mahalu D, Umansky V and Yacoby A 2010 *Nature Physics* **7** 109

[25] Medford J, Cywiński L, Barthel C, Marcus C M, Hanson M P and Gossard A C 2012 *Phys. Rev. Lett.* **108** 086802

[26] de Lange G, Rist D, Dobrovitski V V and Hanson R 2011 *Phys. Rev. Lett.* **106** 080802

[27] Bylander J, Gustavsson S, Yan F, Yoshihara F, Harrabi K, Fitch G, Cory D G, Nakamura Y, Tsai J S and Oliver W D 2011 *Nat. Phys.* **7** 565

[28] Kotler S, Akerman N, Glickman Y, Keselman A and Ozeri R 2011 *Nature* **473** 61

[29] Byrd M and Lidar D 2002 *Quantum Information Processing* **1** 19

[30] Tung W 1985 *Group Theory in Physics* v. 1 (World Scientific)

[31] Schlosshauer M 2008 *Decoherence: and the Quantum-To-Classical Transition* (Springer)

[32] Khodjasteh K and Lidar D A 2008 *Phys. Rev.* A **78** 012355

[33] Khodjasteh K and Viola L 2009 *Phys. Rev.* A **80** 032314

[34] Magnus W 1954 *Communications on Pure and Applied Mathematics* **7** 649

[35] Blanes S, Casas F, Oteo J and Ros J 2009 *Physics Reports* **470** 151

[36] Ng H K, Lidar D A and Preskill J 2011 *Phys. Rev. A* **84** 012305

[37] Nielsen M A 2002 *Phys. Lett.* A **303** 249

[38] Schumacher B 1996 *Phys. Rev.* A **54** 2614

[39] Green T, Uys H and Biercuk M J 2012 *Phys. Rev. Lett.* **109** 020501

[40] Levitt M H 1986 *Prog. NMR Spectrosc.* **18** 61

[41] Merrill J T and Brown K R 2012 *arXiv:1203.6392*

[42] Uhrig G S 2008 *New J. Phys.* **10** 083024

[43] Breuer H and Petruccione F 2002 *The Theory of Open Quantum Systems* (Oxford University Press, USA)

[44] Viola L 2012 *Private communication*

[45] Hayes D, Khodjasteh K, Viola L and Biercuk M J 2011 *Phys. Rev. A* **84** 062323

[46] Carr H Y and Purcell E M 1954 *Phys. Rev.* **94** 630

[47] Hahn E L 1950 *Phys. Rev.* **80** 580

[48] Viola L and Knill E 2003 *Phys. Rev. Lett.* **90** 037901

[49] Khodjasteh K, Biercuk M J and Viola L 2012 *arXiv:1206.6087*